Engineering Fracture Mechanics 319 (2025) 111012

Contents lists available at ScienceDirect

Engineering Fracture Mechanics

journal homepage: www.elsevier.com/locate/engfracmech

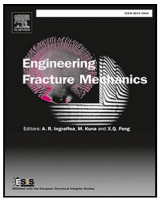

New method for crack length determination in low-temperature DCB tests based on electrical capacitance

Tobias Tiedemann *, Florian Chen, Bodo Fiedler

Institute of Polymer Composites at Hamburg University of Technology, Denickestraße 15, Hamburg, 21073, Germany

ARTICLE INFO

Keywords:
Mode I
GFRP
Fracture toughness
Energy release rate
Composites
Double cantilever beam

ABSTRACT

The double cantilever beam (DCB) test is a widely used method to evaluate interlaminar fractures in composite materials. However, conducting DCB tests at low temperatures reveals challenges, particularly in detecting and characterizing delaminations due to freezing of the specimen. This study proposes a novel approach to address this issue by employing capacitance measurements to identify and quantify delamination growth during DCB tests under low-temperature conditions. Different methods of evaluation are considered and compared in this paper. The results show that reliable results can be determined with the new measurement method and that the process is significantly less susceptible to human error than the usual evaluation methods. This work improves the accuracy and reliability of DCB tests under extreme environmental conditions and has the potential to support the development and application of composite materials in challenging environments like liquid hydrogen storage applications.

1. Introduction

Delamination poses a significant risk to the structural integrity and performance of fiber-reinforced composites. To assess Mode I delamination and determine the critical energy release rate, an important material property, the double cantilever beam test is widely used. Over the years, various methods for testing and evaluation have been established [1,2]. In these tests, a specimen primarily comprised of unidirectional prepreg layers is prepared with a thin non-adhesive film to initiate a sharp crack. Under Mode I loading, as shown in Fig. 1, the specimen is pulled apart, causing the crack to propagate along the fiber direction between the layers of the composite. This causes a delamination between the layers. During the test the applied force and crack opening displacement is measured digitally.

The ASTM 5528 provides comprehensive guidelines for conducting the double cantilever beam test and recommends various evaluation methods [3]. Among these, the *Modified Compliance Calibration Method* stands out for its real-time crack propagation monitoring and continuous assessment of fracture behavior. By accounting for specimen compliance and geometry, this method enhances accuracy. Visual markings on the specimen assist in detecting crack propagation during the test, aiding in the construction of material-specific Crack Resistance Curves (R-Curves).

The R-curve, illustrated in Fig. 2, depicts the energy release rate over the crack length. In composites, it typically consists of two stages: a propagation stage and a saturation stage. When the critical energy release rate G_{I_c} is reached in the specimen due to external loading, crack initiation occurs. During the propagation stage, the energy release rate increases, driven by various factors depending on the material being investigated. For ductile materials, energy is consumed in creating plastic deformation ahead of the crack, while in brittle composites, the fiber bridging effect predominates. Typically, the energy release rate does not surpass

* Corresponding author.
E-mail address: tobias.tiedemann@tuhh.de (T. Tiedemann).

https://doi.org/10.1016/j.engfracmech.2025.111012
Received 17 June 2024; Received in revised form 16 January 2025; Accepted 2 March 2025
Available online 9 March 2025

Nomenclature

Latin symbols

a	Crack length
a_c	Critical crack length
a_{max}	Maximum crack length
a_s	Saturation crack length
b	Width
C	Compliance
C_{el}	Electrical Capacitance
d	Thickness
d_{PTFE}	Thickness of PTFE Layer
E	Young's Modulus
G_{Ic}	Critical Energy Release Rate
G_{Is}	Saturation value of Energy Release Rate
G_I	Energy Release Rate
I	Area Moment of Inertia
P	Force

Greek symbols

δ	Displacement
ϵ_0	Permittivity Constant
ϵ_{Air}	Relative Permittivity of Air
ϵ_{GFRP}	Relative Permittivity of GFRP
ϵ_{CFRP}	Relative Permittivity of CFRP
ϵ_{PTFE}	Relative Permittivity of PTFE

Abbreviations

CFRP	Carbon Fiber Reinforced Polymer
DCB	Double Cantilever Beam
DETDA	Diethyltoluoldiamin
DGEBA	Bisphenol-A-diglycidylether
GFRP	Glass Fiber Reinforced Polymer
MCC	Modified Compliance Calibration
PTFE	Polytetrafluorethylen

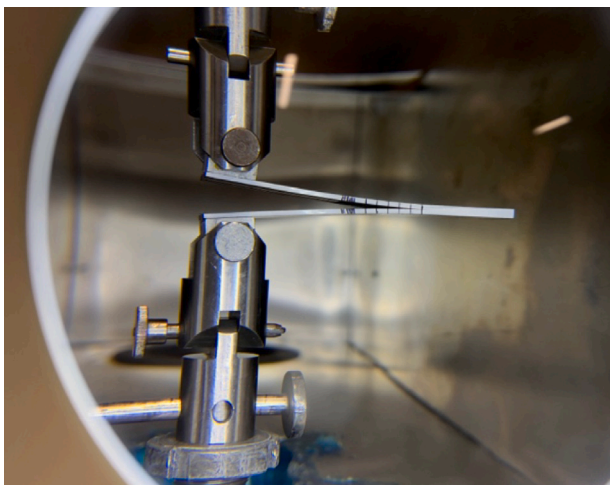

Fig. 1. Photo of DCB Test setup.

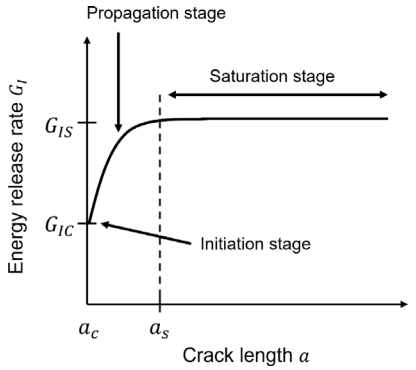

Fig. 2. Theoretical crack resistance curve for a composite material. Modified after [6].

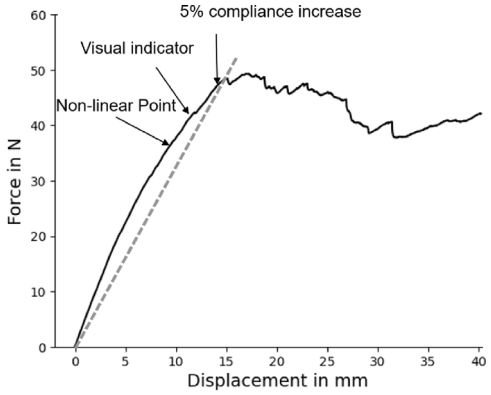

Fig. 3. Schematic illustration of the crack initiation point definition.

a certain threshold value, G_{I_S}. Factors such as the maximum size of the plastic zone or the maximum amount of fiber bridging associated with the crack may be responsible for this limitation [4,5]. The R-curve provides insights into material behavior during both crack initiation (G_{I_c}) and steady-state crack growth (G_{I_s}).

The precision of measurement strongly depends on the accuracy of the crack length detection using visual markers on the specimen. These methodologies facilitate the determination of the critical energy release rate based on the force–displacement data. Various approaches for determining the critical energy release rate were analyzed in round robin tests [7]. These approaches include utilizing the first non-linear point in the force–displacement curve or an increasing compliance by 5% after the onset of the non-linear point. Results showed that none of these methods exhibited inherent superiority over others in determining the critical energy release rate. However, employing all methods introduced inaccuracies and a scatter of approximately ±10% in round robin tests [7]. Fig. 3 illustrates the crack starting points determined using different methods.

Environmental factors, such as elevated humidity and temperature, significantly impact delamination characteristics of composites [8]. As composite materials are increasingly utilized in novel applications like liquid hydrogen transport and storage, understanding their fracture behavior at low temperatures becomes more important [9]. However, conventional crack length determination methods using visual markings become impractical at low temperatures due to humidity that is freezing on the specimen, as illustrated in Fig. 4.

This challenge necessitates alternative approaches that eliminate the need for specimen visibility during testing. In this study, a novel method for crack length determination is proposed, where specimens are equipped with two copper electrodes to measure the change in electrical capacitance during the test. A similar technique has been explored previously by Bosbach et al. for structural health monitoring of fiber metal laminates [10], the new approach simplifies the process by using copper tape attached to the outside of the specimen and measuring capacitance with a multimeter. This opens up the possibility of using this method for normal composite laminates that are not reinforced with metal layers. A schematic drawing of the setup is sown in Fig. 5.

An electromagnetic field is established between the copper electrodes, behaving ideally like a plate capacitor. Eq. (1) can be utilized to calculate the capacitance of a plate capacitor C_{el}, with the capacitance being influenced by factors such as the relative permittivity of air ϵ_{Air} the materials $\epsilon_{Composite}$ and geometric parameters like width b and distance d.

$$C_{el} = \epsilon_0 \cdot (\epsilon_{Air} \cdot a + \epsilon_{Composite} \cdot (a_{max} - a)) \frac{b}{d} \tag{1}$$

Fig. 4. Frozen humidity on the DCB specimen during low temperature testing.

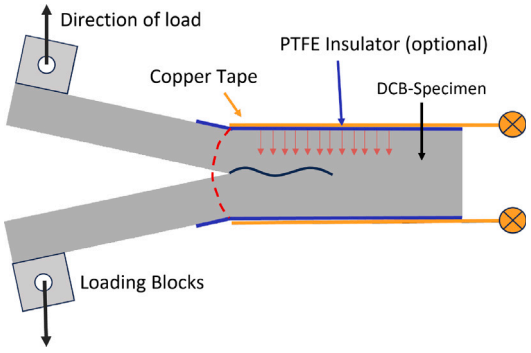

Fig. 5. Schematic illustration capacitance measurement test setup.

Eq. (1) and Fig. 5 can be employed to illustrate the correlation between capacitance and crack length. At the onset of the test, when the crack length a is zero, only the relative permittivity of the composite material is considered. Consequently, as crack propagation initiates and a increases, the proportion of the crack (assumed to have the relative permittivity of air) grows while the proportion of the composite diminishes. Consequently, the capacitance in the capacitor decreases with the increasing crack length. Throughout this process, the area in the capacitor remains constant, and changes in distance d, which is defined by the thickness of the specimen, are neglected. The deflection of the specimen during the test, while the crack runs through the material, leads to an increase in the distance d between the electrodes and to a non-parallel arrangement of the electrodes. However, Bueno-Barrachina et al. [11] have demonstrated that at small angles, the non-parallelism of a capacitor has a negligible influence on the capacitance. The change in permittivity due to the increase in crack size is significantly greater in the measurement. For this reason, non-parallelism is disregarded and a permanently parallel capacitor is assumed. To test conductive Materials like Carbon fiber reinforced polymers (CFRP) a thin layer of PTFE Tape can be added between the copper tape and the specimen for electrical insulation.

In the case of using an additional PTFE film for CFRP specimens, an additional term $\epsilon_{PTFE} \cdot a_{max}$ is introduced in Eq. (1) resulting in Eq. (2). Importantly, this term is independent of the crack length and only impacts the absolute value of the capacitance. The crack length measurement is not effected, since the relative change of the capacitance during the measurement is used for the evaluation.

$$C_{el} = \epsilon_0 \cdot (\epsilon_{Air} \cdot a + \epsilon_{Composite} \cdot (a_{max} - a)) \cdot \frac{b}{d} + \epsilon_0 \cdot \epsilon_{PTFE} \cdot a_{max} \cdot \frac{b}{d_{PTFE}} \tag{2}$$

Some literature values for the permittivity of the used materials are shown in Table 1. The difference in permittivity between the air and the tested material is decisive for the sensitivity of the measurement.

The crack length can be determined during the test using capacitance measurement by monitoring the relative change in capacitance over the duration of the test. At the start of the measurement, the crack length is assumed to be 0 mm, and at the end of the measurement, a_{max} is assumed to be the crack length. The crack length can be calculated using the linear relationship from Eq. (1) or Eq. (2) respectively.

Other authors have previously presented methods that also aim to replace the manual reading of the crack length with visual markings. Wang et al. presented a method in which a guided wave is sent through the specimen with the aid of piezoelectric sensors attached to it [16]. The onset of crack propagation can be determined based on the change in this wave signal during the test. However, a determination of the crack length during the test was not carried out in that work. An alternative approach is

Table 1
Permittivity values.

Material	Absolute/relative permittivity	Source
ϵ_0	$8.85 \cdot 10^{-12}$ F/m	[12]
ϵ_{Air}	1	[13]
ϵ_{GFRP}	4...4.8	[14]
ϵ_{CFRP}	50...56	Own measurements
ϵ_{PTFE}	2	[15]

to calculate the crack length using beam theory [17]. This assumes that the specimen is firmly clamped on one side and pulled upwards on the other side. The length of the beam then corresponds to the crack length in the DCB specimen. The crack length can then be determined using Eq. (3). This requires the Young's modulus E of the material and the area moment of inertia I, which can be calculated from the specimen geometry. P describes the force acting on the specimen.

$$a = \sqrt[3]{\frac{\frac{\delta}{2} \cdot 3 \cdot E \cdot I}{P}} \tag{3}$$

The primary disadvantage of this method is that it is only valid for small angles. Furthermore, studies have demonstrated that the MCC method, which is commonly used today, is more accurate than this approach.

This study aims to evaluate the critical energy release rate and the crack resistance curve of two composite materials (GFRP and CFRP) using the double cantilever beam test. Room temperature tests use the ASTM 5528 guidelines, employing both visual and capacitance-based crack length determination methods. In low-temperature testing, crack length is determined through capacitance measurement.

2. Materials

The materials utilized in this study include unidirectional glass fibers with an areal weight of 600 g/m^2 (Interglas GmbH, Erbach, Germany (Now Porcher Industries)), serving as the primary reinforcement component. For the matrix, an unmodified Bisphenol-A-diglycidylether (DGEBA) epoxy resin Epikote 828LVEL (Westlake, USA) was employed, along with H81b (Schill + Seilacher GmbH, Hamburg, Germany) as the Diethyltoluoldiamin (DETDA) curing agent, accelerated with salicylic acid. To initiate the initial crack in the specimen, a 10 µm thin non-adhesive PTFE film (Goodfellow, UK) was positioned in the middle of the ply layup, which comprised ten unidirectional layers. The selection of glass fiber material was driven by its non-conductive properties. Furthermore, to investigate the method with conductive materials, carbon fiber prepreg material M21-T800S (Hexcel, Stade Germany) was utilized for comparative analysis.

Specimen Production

For the manufacturing of the test specimens, prepregs were initially manufactured from the glass fibers using the in-house developed Direct Preg process. This step was unnecessary for the CFRP materials, as they were readily available as prepregs.

To ensure a homogeneous mixture, the epoxy resin was stirred with the curing agent for 15 min at a speed of 200 rpm under vacuum.

The resin mixture was then processed into prepreg sheets using an impregnation roll mill using the Direg Preg process. This process involved applying the resin onto two rotating rollers, thereby creating an evenly distributed matrix on the rollers. The distance between the rollers is adjusted to control the amount of resin applied to the fibers. Layer by layer, the fibers were added onto the rollers, ensuring even distribution of the resin without any dry spots. The resulting prepregs sheets had a fiber volume content of $52\% \pm 2\%$, confirming the uniform distribution of fibers within the composite. After the impregnation, the prepregs were stacked to form ten layers with a thickness of approximately 4 mm. A non-adhesive 10 µm PTFE film is inserted into the middle layer on one half of the plate to create the precrack necessary for the DCB specimen geometry as indented in ASTM 5528. Curing is performed in an autoclave subjecting the specimens to a pressure of 7 bars while maintaining a temperature of 80 °C for 4 h, followed by an additional 4 h curing step at 140 °C. Similarly, the CFRP prepregs for the comparison specimens were laminated. Here, 16 layers were utilized to achieve a material thickness of 4 mm due to the lower layer thickness (0.262 mm). These materials were then cured in a separate autoclave process at 180 °C and 7 bars, following the manufacturer's specifications. Once cured, the panels were trimmed using a sliding table saw and cut to the required specimen sizes using a precision saw (ATM Brilliant 250). The sides of the specimens were sprayed with white paint, and distances from the film were marked at increments of one millimeter within the first five millimeters and every five millimeters thereafter to track the direction of crack development. The specimen geometry and dimensions are shown in Fig. 6.

3. Methods

The experimental methods for this study comprises two main parts: Room temperature tests and the low temperature tests. They are explained separately in the following.

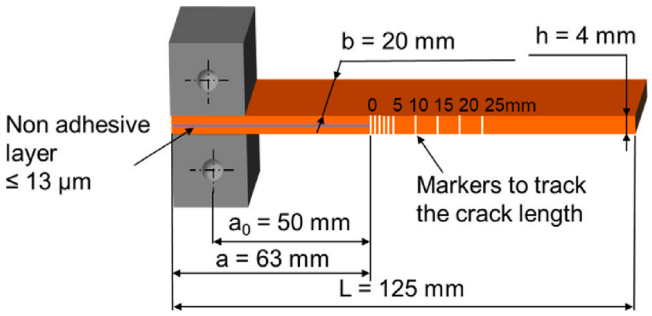

Fig. 6. DCB Specimen dimensions [10].

Room temperature tests

The room temperature tests are carried out according to the ASTM 5528 Standard, with a minor modification involving the use of copper tape adhered to the top and bottom of the specimen, serving as electrodes for capacitance measurements. Otherwise, the specimens remain unmodified. After carefully inserting the specimen into the testing machine (Zwick Z010, Ulm, Germany), the force has been zeroed. The test commences with the controlled opening of the laminate at a rate of 2 mm/min. Visible markers along the sides of the specimens facilitate the visual tracking of crack length during the test. Simultaneously, the capacitance between the two applied copper tape stripes is measured and recorded using an LCR Meter (Peaktech P2170) at a frequency of 10 kHz. Whenever the propagating crack intersects one of the markers, several parameters are recorded, including the applied force, displacement, capacitance, and the current crack length. The test progresses until the full breakage of the specimen. Following the *Modified Compliance Calibration* method, the compliance (C) is initially calculated as $C = \frac{P}{\delta}$, where P is the applied force and δ is the displacement. Subsequently, a plot of $\frac{a}{h}$ over $C^{1/3}$ is constructed. The slope (A_1) of this linear correlation is then utilized for the calculation of the Energy Release Rate (G_I) with Eq. (4).

$$G_I = \frac{3 \cdot P^2 \cdot C^{2/3}}{2 \cdot A_1 \cdot b \cdot h} \tag{4}$$

Using this method, the critical energy release rate G_{I_c} is identified as the initial data point when crack propagation initiates. The progression of G_I over the crack length a delineates the crack-resistance curve as a material parameter.

Low temperature test

The second phase of the experiments involves conducting DCB tests at low temperatures. To achieve this, the test specimens and the entire test setup are cooled using cold air from an external cooling unit. The cold air is supplied via insulated hoses into an insulated test chamber where the test setup is located. Following a pre-cooling period of 30 min, both the specimens and the setup stabilize at a constant temperature of −40 °C. Notably, ice crystals form on the specimen, rendering the markings no longer visible. During the cooling process, changes in capacitance were measured, revealing a linear reduction of 0.02 pF per ° C. A reason for this can be a change in the permittivity of the materials, the reduced humidity in the surrounding air while cooling or (to a lesser extent) the thermal contraction of the materials.

Once the constant temperature of −40 °C is reached, the test begins. Unlike the room temperature tests, where individual data points are recorded as the crack crosses the markings, in the low-temperature test, capacitance is measured continuously alongside force and displacement. To overcome the temperature dependence of the capacitance, the values of the capacitance measurement were normalized by the starting value of the measurement for the evaluation.

The tests at both room temperature and low temperatures were conducted using five specimens each of two material configurations. One material configuration comprises the glass fiber laminate, while the second consists of carbon fiber material. The latter configuration is electrically conductive because of the carbon fibers. This necessitates the use of an additional electrical insulation layer made from PTFE tape beneath the copper tape to prevent contact between the copper tape and the specimen.

Capacitance Measurement

Analysis of the data collected from the room temperature test reveals a clear linear relationship between crack length and capacitance. This information serves as a crucial baseline for the study.

Copper tape is carefully affixed to the top and bottom center of the specimen without any folds. The leading edge of the copper tape starts at the point where the non-adhesive film ends and the first mark is applied. The tape extends approximately 10 mm beyond the specimen to accommodate the attachment of contacts for the measuring device. To ensure they do not affect the capacitance measurement, the ends are bent upwards by 90°. Fig. 5 provides a schematic of the capacitance measurement setup.

It is important to position the copper tape correctly, adhering it only up to the end of the inserted film. Extending the tape beyond this point would result in an invalid model of the ideal plate capacitor. The front area of the specimen with the pre-crack experiences significant deflection due to lower bending stiffness. Consequently, the capacitance in this area decreases sharply even without any crack propagation. Fig. 7 compares measurements taken with long and short versions of the copper tape. The non-linear behavior in the capacitance measurement on the left-hand side is clearly recognizable (see Fig. 7 cicled in orange).

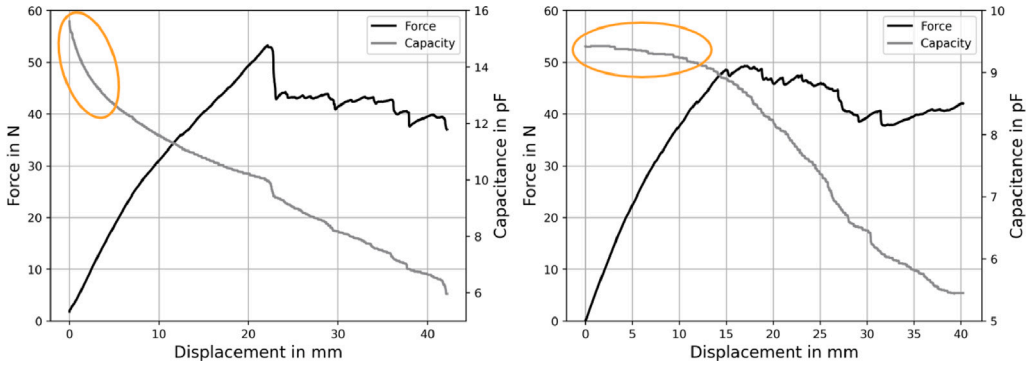

Fig. 7. Left: Test result with long copper tape. Right: Test result with short tape.

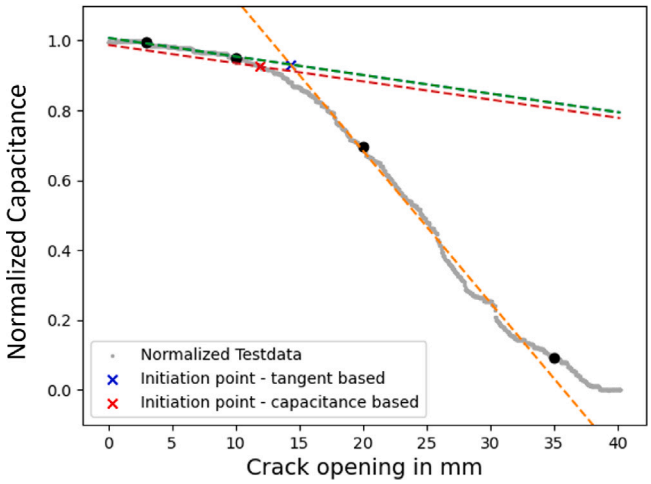

Fig. 8. Illustration of the two newly introduced methods to investigate the onset of the crack growth using capacitance measurement.

By placing the copper tape at the start point of the crack, the capacitance measurement introduces new evaluation possibilities for determining the crack initiation point and thus G_{IC}. Different approaches are shown in Fig. 8. One approach is to utilize the gradient of the capacitance; crack initiation can be defined similarly to the compliance method, at a reduction of 5%. Another approach is to use a tangential construction in the linear region at the beginning of the test and during crack propagation. The intersection of these two tangents can be used to define the initiation of the crack. These methods are both mathematical, offering the advantage of easy automation. This reduces the human error associated with visual crack tracking compared to the visual investigation of crack growth [1]. It is known from literature, that the crack in the specimen does not develop in a straight line. It can happen, that the crack front is curved like in Fig. 9 shown. This can also influence the visual detection of the crack length. The new method has the advantage of placing the electrodes freely on the surface of the specimen.

The method necessitates data on both the crack initiation point and the endpoint of the measurement to correlate the capacitance with the crack length. The endpoint is relatively straightforward to determine if the specimen is tested to failure to ascertain a_{max}. Regarding the initial crack, ASTM 5528 offers three methods: the non-linear point, visual inspection, and a 5% compliance increase. With the capacitance measurement method, two alternative methods for determining the crack initiation point are the 5% capacitance decrease and the tangent method. Since the linear regression of capacitance over crack length is defined between two points in the absence of information from the visual method for determining crack length, identifying the correct starting point is crucial for measurement accuracy. After defining the starting point and establishing the capacitance/crack length relationship, the standard *Modified Compliance Calibration Method* from ASTM 5528 can be employed to plot the compliance graph, compute the slope, and calculate G_I using Eq. (4). In this work, GFRP and CFRP specimens were analyzed for their energy release rate in order to test the functionality of the method. Subsequently, GFRP specimens were tested at low temperatures and the results were also compared with the tests at room temperature. To validate the results, the beam theory was used with Eq. (3) to compare the calculation of the crack length with the calculation from the capacitance measurement.

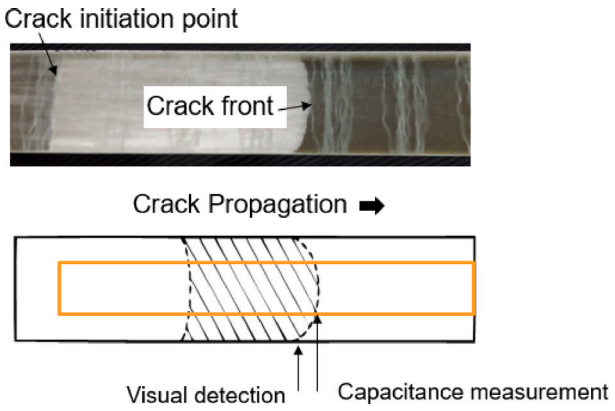

Fig. 9. Schematic drawing of the crack propagation with a photo from [18].

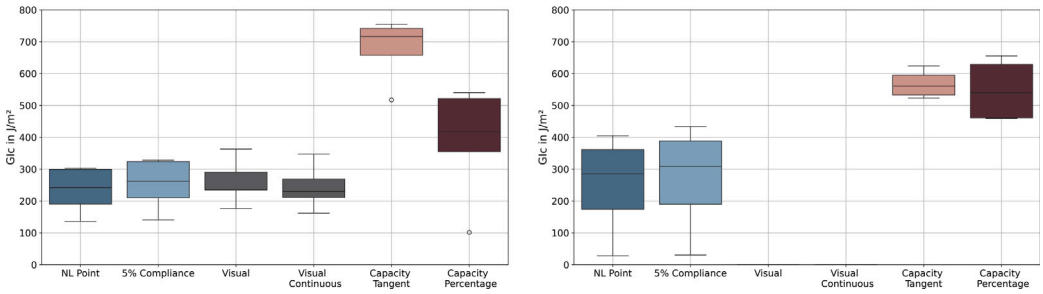

Fig. 10. Left: Critical energy release rate of tested GFRP materials at room temperature. Right: −40 °C Test temperature.

4. Results

This section presents the study results, which aim to validate the measurement method and demonstrate the feasibility across different materials. The emphasis is not placed on the specific material values but rather on the comparative analysis. For each specimen, the crack initiation point was determined using the aforementioned methods, and the critical energy release rate was calculated using the MCC method. Fig. 10 illustrates the results of G_{Ic} determination for GFRP at room temperature and at a test temperature of −40 °C. It is evident that the standard methods utilizing the nonlinear point, the 5% compliance decrease, and the visual marker method exhibit a closely clustered range of values within their standard deviation. Conversely, the novel methods employing capacitance measurement with capacitance decrease and the tangent method yield notably higher values for G_{Ic}, attributed to delayed crack initiation detection. It should be noted that the evaluation method using the tangent construction is more dependent on the specimen's stiffness. GFRP specimens tend to exhibit more bending during tests, which introduces non-linearity into the capacitance measurement and has the strongest effect on this method. Conversely, cold temperatures result in increased material stiffness and reduced non-linearity. It is also evident that CFRP materials with higher stiffness exhibit lower GIC values when measured using the Capacitance Tangent method. Notably, visual methods cannot be utilized at low temperatures due to the absence of visible markings. This means that some adjustments still need to be made to the GFRP measurements with regard to the detection of crack initiation. For example, the 5% reduction in capacitance can also be triggered at a lower percentage if this is desired.

In contrast, the results of the CFRP investigation depicted in Fig. 11 demonstrate superior performance of the capacitance measurement methods. Additionally, the standard crack initiation methods also exhibit a lower standard deviation. This discrepancy can be attributed to the higher stiffness of the CFRP material, resulting in reduced deflection of the specimen halves. Consequently, the force displacement curve maintains linearity over an extended range. In contrast, the GFRP results exhibit non-linearity before crack initiation, which renders the evaluation methods more sensitive.

The following Fig. 12 presents a representative R-curve for GFRP specimens measured at room temperature. The data points represent the energy release rate determined by visual crack length determination according to ASTM 5528. The solid gray line represents the capacitance measurement and the resulting crack length. Notably, the same starting point was used for both the visual measurement and the capacitance measurement. The third dataset depicted in red illustrates the results when the starting point was determined using the 5% capacitance decrease method. This example vividly demonstrates the variation in energy release

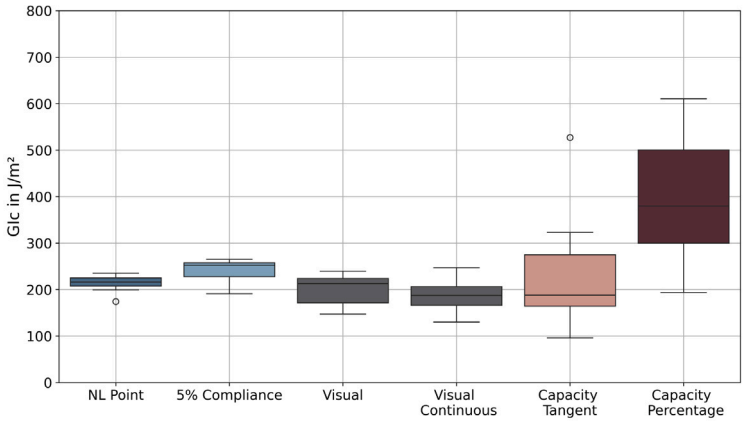

Fig. 11. Critical energy release rate of tested CFRP materials at room temperature.

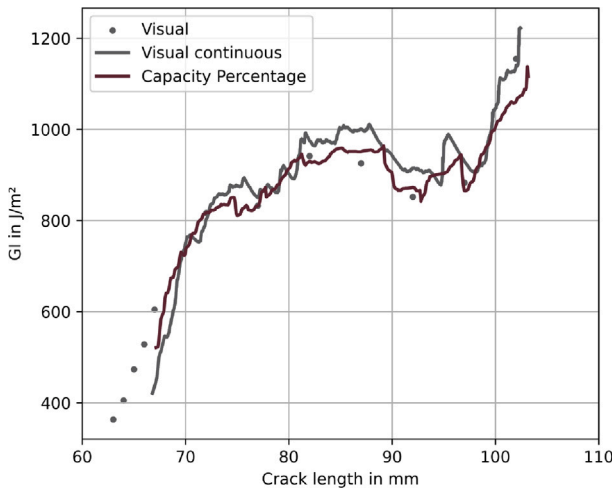

Fig. 12. Crack resistance curve of a representative GFRP specimen.

rate depending on the selected starting point. However, it also shows that the new method can be used to generate a continuous measurement curve for the R-curve and that more data points are available than for purely visual measurement. The deviations of the R-curve are within a 10% confidence interval and are therefore no greater than with the standard method.

5. Conclusion

In summary, the new method offers a reliable approach to constructing a crack resistance curve from DCB measurement data. Despite its dependence on the initial crack, the resulting deviations in the R-curve are comparable in magnitude to those caused by other measurement methods already incorporated in the standard. The efficacy of the new capacitance-based methods for determining crack initiation is subject to debate; however, they have demonstrated effectiveness with CFRP material. Nonetheless, the standard methods remain applicable. Moreover, continuous capacitance measurement provides additional data points, leading to a more precise depiction of the fracture behavior of the DCB specimen. The method facilitates testing of DCB specimens in a closed environment without a clear view of the markings on the specimen side. Evaluation is conducted using the MCC method, known for its accuracy. Another advantage is the ability of capacitance measurement to offer additional insights into the progression of the crack front. It is well-established that the crack advances in the center of the specimen and reaches the markings at the edge of the specimen somewhat later [18]. The new method enables detailed measurement of the crack front, potentially surpassing the standard MCC method.

CRediT authorship contribution statement

Tobias Tiedemann: Writing – original draft, Visualization, Methodology, Formal analysis. **Florian Chen:** Visualization, Formal analysis, Data curation. **Bodo Fiedler:** Supervision, Methodology.

Declaration of competing interest

The authors declare the following financial interests/personal relationships which may be considered as potential competing interests: The authors declare that they have no known competing financial interests or personal relationships that could have appeared to influence the work reported in this paper.

Acknowledgments

Publishing fees were supported by DFG Project 513556749. The authors would like to thank the Ingeborg-Gross-Foundation for financial support, Schill + Seilacher and Westlake Epoxy for the cost-neutral supply of material.

Data availability

Data will be made available on request.

References

[1] Brunner AJ. Fracture mechanics testing of fiber-reinforced polymer composites: The effects of the “human factor” on repeatability and reproducibility of test data. Eng Fract Mech 2022;264:108340. http://dx.doi.org/10.1016/j.engfracmech.2022.108340.
[2] O’Brien T. Interlaminar fracture toughness: the long and winding road to standardization. Compos Part B: Eng 1998;29(1):57–62. http://dx.doi.org/10.1016/S1359-8368(97)00013-9.
[3] D30 Committee. Test method for mode I interlaminar fracture toughness of unidirectional fiber-reinforced polymer matrix composites. Tech. rep., ASTM International, http://dx.doi.org/10.1520/D5528-13.
[4] Russo A, Zarrelli M, Sellitto A, Riccio A. Fiber bridging induced toughening effects on the delamination behavior of composite stiffened panels under bending loading: A numerical/experimental study. Materials 2019;12(15):2407. http://dx.doi.org/10.3390/ma12152407.
[5] Sørensen BF, Jacobsen TK. Large-scale bridging in composites: R-curves and bridging laws. Compos Part A: Appl Sci Manuf 1998;29(11):1443–51. http://dx.doi.org/10.1016/S1359-835X(98)00025-6.
[6] Heidari-Rarani M, Shokrieh MM, Camanho PP. Finite element modeling of mode I delamination growth in laminated DCB specimens with *R*-curve effects. Compos Part B: Eng 2013;45(1):897–903. http://dx.doi.org/10.1016/j.compositesb.2012.09.051.
[7] Davies P, Kausch H, Williams J, Kinloch A, Charalambides M, Pavan A, Moore D, Prediger R, Robinson I, Burgoyne N, Friedrich K, Wittich H, Rebelo C, Torres Marques A, Ramsteiner F, Melve B, Fischer M, Roux N, Martin D, Czarnocki P, Neville D, Verpoest I, Goffaux B, Lee R, Walls K, Trigwell N, Partridge I, Jaussaud J, Andersen S, Giraud Y, Hale G, McGrath G. Round-robin interlaminar fracture testing of carbon-fibre-reinforced epoxy and PEEK composites. Compos Sci Technol 1992;43(2):129–36. http://dx.doi.org/10.1016/0266-3538(92)90003-L.
[8] Adler EJ, Martins JR. Hydrogen-powered aircraft: Fundamental concepts, key technologies, and environmental impacts. Prog Aerosp Sci 2023;141:100922. http://dx.doi.org/10.1016/j.paerosci.2023.100922.
[9] Timmerman JF, Tillman MS, Hayes BS, Seferis JC. Matrix and Fiber influencess on the cryogenic microcracking of carbon Fiber/epoxy composites. Compos Part A: Appl Sci Manuf 2002;33. 328.
[10] Bosbach B, Ohle C, Fiedler B. Structural health monitoring of fibre metal laminates under mode I and II loading. Compos Part A: Appl Sci Manuf 2018;107:471–8. http://dx.doi.org/10.1016/j.compositesa.2018.01.008.
[11] Bueno-Barrachina, Cafias-Pefiuelas, Catalan-Izquierdo. Capacitance evaluation on non-parallel thick-plate capacitors by means of finite element analysis. 2011, URL https://api.semanticscholar.org/CorpusID:54782973.
[12] CODATA Value: vacuum electric permittivity. 2024, URL https://physics.nist.gov/cgi-bin/cuu/Value?ep0.
[13] Scott K. Permittivity. 2024, http://dx.doi.org/10.1615/AtoZ.p.permittivity, URL https://www.thermopedia.com/content/1018/.
[14] Li Z, Haigh A, Soutis C, Gibson A, Sloan R. Dielectric constant of a three-dimensional woven glass fibre composite: Analysis and measurement. Compos Struct 2017;180:853–61. http://dx.doi.org/10.1016/j.compstruct.2017.08.061.
[15] Shimizu T, Kawahara Y, Akasaka S, Kogami Y. Complex permittivity measurements of a PTFE substrate in w band by the cut-off circular waveguide method. In: 2011 China-Japan joint microwave conference. 2011, p. 1–4.
[16] Wang D, Ye L, Tang Y, Lu Y. Monitoring of delamination onset and growth during Mode I and Mode II interlaminar fracture tests using guided waves. Compos Sci Technol 2012;72(2):145–51. http://dx.doi.org/10.1016/j.compscitech.2011.10.004.
[17] De Gracia J, Boyano A, Arrese A, Mujika F. A new approach for determining the *R*-curve in DCB tests without optical measurements. Eng Fract Mech 2015;135:274–85. http://dx.doi.org/10.1016/j.engfracmech.2015.01.016.
[18] Davidson B. An analytical investigation of delamination front curvature in double cantilever beam specimens. J Compos Mater 1990;24(11):1124–37. http://dx.doi.org/10.1177/002199839002401101.